Available online at www.sciencedirect.com
ScienceDirect
Journal of Power Sources 167 (2007) 340–348
JOURNAL OF POWER SOURCES
www.elsevier.com/locate/jpowsour

Application of sol gel spin coated yttria-stabilized zirconia layers for the improvement of solid oxide fuel cell electrolytes produced by atmospheric plasma spraying

Lars Rose [a,b,*], Olivera Kesler [b,c], Zhaolin Tang [d], Alan Burgess [d]

[a] University of British Columbia, Department of Materials Engineering, 309-6350 Stores Road, Vancouver, British Columbia, V6T 1Z4, Canada
[b] National Research Council, Institute for Fuel Cell Innovation, 4250 Wesbrook Mall, Vancouver, British Columbia, V6T 1W5, Canada
[c] University of British Columbia, Department of Mechanical Engineering, 2054-6250 Applied Science Lane, Vancouver, British Columbia, V6T 1Z4, Canada
[d] Northwest Mettech Corp., 467 Mountain Hwy, North Vancouver, British Columbia, V7J 2L3, Canada

Received 23 November 2006; received in revised form 23 December 2006; accepted 2 January 2007
Available online 6 February 2007

Abstract

Due to its high thermal stability and purely oxide ionic conductivity, yttria-stabilized zirconia (YSZ) is the most commonly used electrolyte material for solid oxide fuel cells (SOFCs). Standard electrolyte fabrication techniques for planar SOFCs involve wet ceramic techniques such as tape-casting or screen printing, requiring sintering steps at temperatures above 1300 °C. Plasma spraying (PS) may provide a more rapid and cost efficient method to produce SOFCs without sintering. High-temperature sintering requires long processing times and can lead to oxidation of metal alloys used as mechanical supports, or to detrimental interreactions between the electrolyte and adjacent electrode layers. This study investigates the use of spin coated sol gel derived YSZ precursor solutions to fill the pores present in plasma sprayed YSZ layers, and to enhance the surface area for reaction at the electrolyte-cathode interface, without the use of high-temperature firing steps. The effects of different plasma conditions and sol concentrations and solid loadings on the gas permeability and fuel cell performance have been investigated.

Keywords: Atmospheric plasma spraying; Sol gel; Spin coating; YSZ; Porosity reduction; OCV

1. Introduction

Fuel cells electrochemically convert the chemical energy in fuels to electrical energy, more efficiently and with much lower pollution than electrical generators based on combustion. Solid oxide fuel cells (SOFCs), with their high (>600 °C) operating temperatures, offer the advantage of high efficiency, especially in co-generation. The capability to use a large selection of fuels, including hydrocarbons and carbon monoxide, also gives SOFCs flexibility not found in low-temperature fuel cells that are poisoned by CO.

SOFC production typically includes wet ceramic techniques, such as tape-casting or extrusion and screen printing or slurry spraying, followed by at least one firing step [1]. Dense YSZ films for SOFCs can also be applied on tubular cells by chemical vapour deposition (CVD) [2]. However, vacuum-based deposition techniques such as CVD are very expensive. Spin coating combined with high-temperature firing steps (1300 °C) can also be used to produce stand-alone YSZ electrolyte layers with low (1–2%) porosity, but only by utilizing lower-conductivity compositions of YSZ that are not fully stabilized [3].

Plasma spraying (PS) is often used for the deposition of electrolyte or ceramic interconnect layers in tubular cells. PS offers the possibility to deposit ceramic, metal, or composite layers, without the need for high-temperature sintering. PS is also an easier method for coating large areas and complex shapes that are difficult to coat with planar wet ceramic deposition techniques. Consequently, PS is uniquely suited for deposition of patterned strip ceramic interconnects on tubular cells that cannot be fired at high-temperatures, to avoid interreactions between cathode and electrolyte.

* Corresponding author at: National Research Council, Institute for Fuel Cell Innovation Canada, 4250 Wesbrook Mall, V6T 1W5 Vancouver, BC, Canada. Tel.: +1 604 2213000x5538; fax: +1 604 2213001.
E-mail address: lars.rose@nrc-cnrc.gc.ca (L. Rose).

0378-7753/$ – see front matter © 2007 Elsevier B.V. All rights reserved.
doi:10.1016/j.jpowsour.2007.01.081

More recently, plasma spraying has been studied as a technique with the potential to deposit all of the electrochemically active fuel cell layers on a low-cost, robust metallic interconnect (IC) support layer with no subsequent high-temperature firing step. This approach reduces the material cost of the fuel cell and minimizes the risk of oxidation of the metallic IC during processing [4]. By avoiding the lengthy high-temperature firing steps, the need for parallel production lines for mass production is also decreased. Material compatibility problems such as interreactions between layers at high sintering temperatures can also be avoided.

PS is a well-established technique to produce both powders and thick (micrometre to millimetre range) coatings [5,6]. Due to the large amount of heat generated in a plasma flame, nearly any material can be coated. Atmospheric plasma spraying (APS), performed in air at atmospheric pressure [7], offers significant advantages over vacuum plasma spraying (VPS). VPS is typically used to produce thin, dense, flat coatings, but can also create porous coatings with up to 15% porosity [8]. The necessity to create and maintain vacuum conditions during deposition increases capital and operating cost of VPS deposition. High gas flow rates through the torch, usually several hundred litres per minute, have to be pumped out of the chambers during deposition. Consequently, this batch processing technique is less favourable for mass production, both in terms of cost and scalability. APS, on the other hand, because it is performed in air under atmospheric pressure, has capital and operating costs that are approximately one order of magnitude lower compared to those of VPS [9].

The properties of PS coating layers vary significantly with feedstock types. Feedstocks can be liquids, powders, or solid rods [10]. For powder based delivery, particle shape, particle size, and size distribution are of importance [11]. Powders that are very small are susceptible to vapourization in the plasma torch or to difficulties with feeding. Large particles may not fully melt in the plasma, and may bounce off the substrate surface if they have remained solid or have re-solidified in flight. The wide range of feedstocks available for plasma spraying provides the process with the flexibility that is required for the spraying of different SOFC layers. These layers can consist of different combinations of materials, with widely varying porosity requirements. This flexibility makes the process potentially more readily adaptable to the fabrication of SOFCs compared to other deposition processes that utilize only one feedstock type.

PS processing is commonly used to create ceramic YSZ coatings for thermal barrier applications, typically with a porosity distribution from 5 to 15% [12]. Denser layers are possible with the use of appropriate spraying and feedstock parameters. For thermal barrier coatings (TBCs) to be effective, a large thermal gradient must exist over only a few hundred micrometer thick YSZ coating [13–15]. Formation of such a thermal gradient is facilitated by the use of porous PS YSZ coatings, since the porosity decreases the thermal conductivity of the coatings. In applying PS to the production of SOFC electrolytes or electrodes containing YSZ, on the other hand, a much more stringently controlled set of spraying conditions is required. Higher porosities are required for sufficient gas flow through the electrodes to ensure high performance and efficiency. Fully dense electrolyte layers that prevent gas crossover are needed to avoid reactant gas mixing. Gas leakage across the electrolyte leads to lower open circuit voltages (OCVs) and fuel combustion, resulting in lower fuel cell performance and efficiency compared to cells with dense electrolytes.

Coatings created by APS are difficult to produce in thin layers that are fully dense as deposited. Multiple methods have therefore been investigated to reduce the porosity of PS YSZ TBCs, and thereby improve their corrosion resistance and thermomechanical stability. Methods previously investigated include laser glazing [16,17], detonation gun spraying [17], phosphate solution sealing [17], drop coating of ceria-doped zirconia sols for sealing [18], silica sol infiltration of PS chromia coatings [19], and spark plasma sintering [20]. Furthermore, water based nitrate solution decomposition after simple specimen immersion [21,22] and forced vacuum impregnation [23] have been used to improve gas tightness of plasma sprayed coatings.

Sol gel (SG) processing is a well known ceramic fabrication technique that generally does not require high-temperature sintering to produce oxide materials. The SG technique is therefore particularly well-suited as a candidate for use in processing materials for SOFC applications [24]. SG processing is regularly used to produce both dense coatings [25] and powder materials [26]. SG processing is also used to produce high surface area components. Therefore, the technique is also potentially suitable for increasing the electrochemical activity of fuel cell electrode-electrolyte interfaces [27].

Spin coating, organic-based sols, and composite sols with suspended powder have not previously been reported to improve plasma sprayed coatings, TBCs, or SOFC electrolytes, nor to enhance the surface area of electrolyte-electrode interfaces. Investigations of the effects of varying sol concentrations and powder loadings have also not been reported previously in these applications. The present study investigates the densification and surface area enhancement of PS SOFC electrolytes on tape-cast NiO/YSZ substrates. Organic-based YSZ sols with varying chemical compositions and composite sol gel (CSG) slurries with varying solid loadings were applied to the PS YSZ layers by spin coating, and the resulting performance changes investigated.

2. Experimental procedure

2.1. NiO/YSZ substrates

NiO-YSZ anode support substrates were tape-cast (Engineering Associates Inc., model ephea223.5.1.T) on mylar sheet. A slurry with a total dry powder loading of 1 kg, with carbon sphere pore formers added to increase anode gas diffusivity, was produced by mixing and ball milling the slurry mixture components listed in Table 1.

The ethanol, toluene and fish oil were ball milled for over 15 h before adding the powders. The full mixture was then ball milled again for 24 h. Prior to tape-casting a 1.2 mm thick tape in a class 1000 cleanroom, the slurry was degassed in vacuum for 30 min. The resulting tape was dried at room temperature for

Table 1
Chemicals used for preparation of NiO-YSZ anode substrates

Chemical	Purpose	Amount [g]
Ethanol (Fisher Scientific)	Solvent	200
Toluene (Fisher, ACS grade)	Solvent	266
Z-3 Fish Oil (R.E. Mistler)	Dispersant	17
YSZ (Tosoh, TZ-8Y)	Ionically conductive phase	404
Green NiO (Inco, Grade F)	Electronically conductive phase	507
Carbon Black (Cancarb, N991 ultra pure)	Pore former	90
Polyvinylbutyral (R.E. Mistler)	Binder	83
Butyl Benzyl Phthalate S-160 (R.E. Mistler)	Plasticiser	116

72 h, followed by a 12 h drying step at 60 °C. Shapes and sizes required for further plasma spray and sol gel production were cut from the tape, according to the tape shrinkage rates determined by tape sintering tests at each sintering temperature studied. The cut tape samples were out-gassed for 2 h each at 100 °C and at 350 °C. They were then pre-sintered at 1000 °C, followed by a sintering and ironing step at either 1250, 1350, or 1400 °C.

2.2. Plasma sprayed layers

Plasma spraying was performed with an axial feed Northwest Mettech Axial III torch (NWM, North Vancouver, Canada). To investigate the effect of initial coating properties on the impact of the sol gel sealing process, two types of YSZ coatings were produced. One coating was sprayed in a high energy hydrogen/nitrogen plasma with a higher potential to melt the YSZ in flight and thus produce denser layers. The other coating was sprayed with a lower energy nitrogen plasma. In order to maximize substrate porosity for subsequent leakage tests, the high energy plasma sprayed layers were coated on substrates sintered at 1250 °C. This resulted in more than 50% of the substrates breaking during deposition. The substrates for deposition in low energy plasma conditions were therefore fired at 1350 °C, resulting in no breakage during deposition. Leakage rates for uncoated substrates fired at both temperatures were found to exceed the range of the leakage testing apparatus at the temperatures studied. Thus, the differences in gas permeability measured between the coatings with and without added SG layers were due to the presence or absence of the SG coatings, and not due to differences in permeation rates through the substrates.

Feedstock powders were fed through a vibrating hopper feeding the powder at a constant rate into a constant carrier gas flow (see Table 2). The coatings were plasma sprayed on round, 2.54 cm diameter, approximately 1 mm thick sintered NiO/YSZ substrates. The feedstock powder used was 5–25 μm fused and crushed YSZ (Sulzer Metco) fed through a multi purpose powder feeder (Thermico, Germany, model CPF-2HP, 11.5 cm inner diameter, maximum vibration). The APS spray parameters used are presented in Table 2.

The NiO/YSZ substrates were mounted on a 300 mm diameter drum. The sample holder allowed for a 1.27 cm diameter disc area to be sprayed through a mask in front of the substrate.

2.3. Sol gel and composite sol gel processing

In this study, sols were prepared by mixing the chemicals listed in Table 3. After adding each chemical, the solution was stirred at 200 rpm for 30 min without heating. The sol

Table 2
APS parameters for electrolyte production from 5 to 25 μm YSZ feedstock

Parameter [unit]	Lower energy PS conditions	Higher energy PS conditions
Plasma gas composition [vol%]	N_2 [100%]	N_2 [75%]/H_2 [25%]
Plasma gas flow rate [slpm]	200	250
Carrier gas composition [vol%]	Ar [100%]	Ar [100%]
Carrier gas flow rate [slpm]	15	6
Powder feed rate [g min^{-1}]	50	100
Vertical passes of spray robot	50	38
Traverse speed [cm s^{-1}]	6.88	3.65
Standoff distance [mm]	130	150
APS torch electrodes	3	3
Power per electrode [kW]	37	48
Torch current per electrode [A]	150	230
Substrate sample holder rotation rate [rpm]	401	364
Deposited YSZ layer thickness [μm]	15	35

Table 3
Sol gel process mixture

Chemical	Weight [g]	Weight [g]	Weight [g]
2 Propanol (Sigma–Aldrich)	50	50	50
Acetyl acetone (Sigma–Aldrich)	2.5	2.5	2.5
Zirconium tetrapropoxide (Sigma–Aldrich)	4	8	16
Distilled water (in-house)	2.5	5	10
Yttrium nitrate hexahydrate (Sigma–Aldrich, 99.9%)	0.84	1.68	3.36
Sample denotation (sol concentration, no solid powder loading)	SG with low ionic concentration	SG with medium ionic concentration	SG with high ionic concentration

gel solution preparation procedure is described in more detail elsewhere [28].

Once all chemicals were added, the solution was left to stir for 12 h. For the composite sol gel (CSG) slurries, the same sols were produced, and 1 wt% of YSZ powder (Tosoh, TZ-8Y) was added. The sample denotations for the composite sol gel slurries follow the ones in Table 3, as low concentration CSG, medium concentration CSG, and high concentration CSG. Solutions with higher solid loadings (2, 3, 5, and 10 wt%) were also prepared, but produced cracked layers during spin coating and drying, and thus were not considered suitable for further study. Sonication experiments with Tosoh powders in suspension determined the need for long (>1 h) sonication times in order to break down the agglomerates. 12 h of sonication in a 50 °C water bath, however, resulted in the gelation of the high sol concentration CSG. The CSG slurries were thus sonicated for 3 h in a water bath at room temperature. The as-prepared SG solutions and CSG slurries were spin coated (Laurell Technologies, WS-400B-6NPP/Lite/10 K) on the YSZ electrolytes produced by low energy PS on the NiO/YSZ substrates, and on bare NiO-YSZ sintered substrates for comparisons of the coating morphology. The YSZ electrolytes sprayed under high energy conditions were impregnated with coatings of the medium concentration SG solution for comparison with the PS coatings produced in the low energy plasma conditions.

The substrates were spun at 3000 rpm for 2 min. 100 μl of sol were applied onto the substrate with a precision pipette (100 μl Eppendorf) every five seconds, for a total of ten times. Sol application was commenced 5 s after starting the rotation with the maximum acceleration of the spin coater. For post-coating drying, the samples were placed for two minutes on a hot plate at 300 °C. In one set of experiments, this procedure was repeated without a firing step to produce multiple sol gel coatings. The samples were then fired to either 500 or 650 °C. In other experiments, only single layers were spin coated and dried and then immediately fired. In each case, the samples were kept for 1 h at the firing temperature.

2.4. Characterization

The thermal characteristics of the sol gel solutions were investigated by thermogravimetric analysis (TGA) and differential thermal analysis (DTA) in a thermal balance (Linseis L81/1750) under flowing air (40 l h^{-1}) up to 1000 °C. A baseline measurement was recorded and automatically deducted from the sample measurement. The sample was heated at a rate of 2 K min^{-1}. The thermocouple (Type B) used in the experiments is capable of measurements up to 1750 °C, but does not produce reliable data below 100 °C.

The crystallographic evolution of the sol gel solutions was investigated by X-ray diffractometry (XRD, Rigaku). Medium concentration SG solution was dried for 2 h at 150 °C, then ground into a powder and compacted into a Ni pan sample holder for a high-temperature stage, with Ni ribs to allow for good heat contact and distribution during heating. Holder and sample were placed on the heating stage and heated at a rate of 20 K min^{-1}, in steps of 50 °C. After allowing the system to settle for 30 min, an XRD spectrum was recorded at each temperature from 150 to 1000 °C, within a diffraction angle 2θ range of 20–80°.

The sample gas tightness was tested in a sealed rig designed in-house at the National Research Council Institute for Fuel Cell Innovation (NRC-IFCI) for 2.54 cm diameter button cells. Helium gas with a constant pressure (Alicat Scientific PCD Series Digital Pressure Controller, ±0.4% precision) was applied to the substrate. The incoming gas stream was delivered to the electrolyte surface through a rubber o-ring seal with a diameter of 0.95 cm. The permeating gas volume was measured (Alicat Scientific M Series Digital) to determine the ability of the specimens to separate gases under pressure. The gas tightness was tested on sintered substrates, as-sprayed PS coated pellets, and spin coated pellets.

Surface and cross-section views of the samples were investigated by electron microscopy (Hitachi S-3000 and S-3500) to determine the effect of the coating procedures on the material microstructure and morphology. The cross-sections of the full cells were prepared by mounting the cells in conductive thermoset resin, then cutting the sample with a 400 μm diamond saw. The surface was polished with pastes of decreasing mean abrasive particle diameters, ending with a surface finish obtained with a 0.05 μm Al_2O_3 solution.

Composite $Sm_{0.5}Sr_{0.5}CoO_{3-y}$ (SSC)–$Sm_{0.2}Ce_{0.8}O_{3-y}$ SDC (40/60 wt%) cathode slurries were applied through a 0.96 cm opening in a polymer mask using a spatula. The cathode was sintered ex situ at 900 °C for 4 h. The parts of the cell not covered by PS electrolyte on the cathode-side top surface were sealed with YSZ-thermally matched Ceramabond (Aremco), dried for 1 h at room temperature, 2 h at 90 °C, 2 h at 200 °C, and 2 h at 500 °C. These cells were then mounted in a horizontal 2.54 cm diameter test station. The anode was sealed with an alumina felt, and the sides of the cells were not coated with a sealant. Previous electrochemical testing using different sealing methods showed that using ceramic felts typically results in cell open circuit voltages approximately 40 mV lower than in fully (glass-)sealed cells [29].

The cell was reduced with a stepwise (20 vol% per step) increase in hydrogen flow from 0 to 100 vol%. For the electrochemical tests, pure hydrogen was bubbled through water at room temperature (approximately 20 °C). Hydrogen and air flow rates were 100 standard cubic centimetres per minute (sccm). Open circuit potential measurements and full cell polarization and impedance tests were performed at 800, 750, and 700 °C, using a Solartron 1260 Frequency Response Analyzer coupled with a Solartron 1470E Multistat (London Scientific, Canada). The impedance response of the system was recorded from 0.1

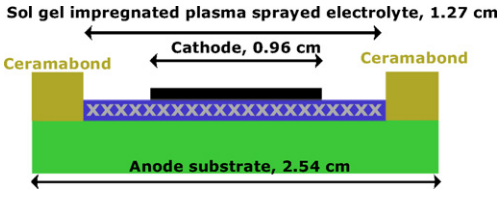

Fig. 1. Principal cross-section of the cells tested during this study.

to 10 kHz. Fig. 1 shows a diagram of the principal cross-section of the produced cells.

3. Results and discussion

Tape sintering shrinkage was found to be 16.72, 20.05, and 26.25% for tapes sintered at 1250, 1350, and 1400 °C, respectively. Substrates with any visible curvature tended to break more easily during PS deposition, and coatings deposited on them tended to have both higher surface roughness and a larger variation in coating thickness across the surface. Furthermore, sealing of curved cells in a test station was difficult to achieve. Consequently, the tape-cast substrates were ironed under a constant load at their sintering temperature for subsequent depositions. None of the samples ironed and sintered at 1350 °C broke during spraying or during any of the subsequent testing. The deposition thickness was found to be constant over the entire deposited layer area.

Dense YSZ layers were not obtained directly on sintered NiO/YSZ substrates by spin coating. The application of large numbers of spin coated sol gel layers with higher sol concentrations resulted in the formation of a separate spin coated YSZ layer that is not fully dense on the surface of the PS YSZ layer. Fig. 2 shows the cross-sections of YSZ layers produced in a high energy plasma with five sol gel coatings (A) and 10 sol gel coatings (B) of medium concentration applied by spin coating. After five coatings, a thin film, morphologically distinct from the PS YSZ coating layer, began to appear on the surface. No surface film was observed after fewer coatings at the available resolution. The micrographs in Fig. 2 suggest that five or more spin coated layers lead to the formation of a separate surface layer on top of the PS layer, rather than only densifying the previously deposited layers by infiltration. This is a positive result from the view of process simplification, since the application of too many layers in post processing makes any treatment less interesting for practical applications. Consequently, the gas permeation was only measured for coatings produced with up to five applied sol gel coatings.

Medium concentration sols also produced cracked layers after firing that were evident in the surface top view when deposited directly on the NiO/YSZ substrate. No such layer was observed on top of the PS electrolyte in the SEM surface micrographs, indicating that the sol infiltrated the electrolyte. Composite sol gel solutions, however, produced separate discontinuous layers after spin coating on both the NiO/YSZ and the PS YSZ electrolytes. This effect was more pronounced for both high sol concentrations and for high (>1 wt%) powder loadings.

Gas permeation testing with helium showed that both the 35 μm PS YSZ layers produced in a high energy plasma and the thinner 15 μm electrolytes sprayed in low energy plasma conditions were not gas tight. Average helium leakage rates at 1 pound per square inch gauge (psig) were 0.30 sccm for YSZ coated in the former conditions, and 0.32 sccm for YSZ coated in the latter conditions. Both substrates sintered at 1250 and 1350 °C had a permeation rate exceeding the instrument measurement limit of 0.64 sccm at 1 psig and consequently negligible influence on gas permeation measurements with applied PS layers.

Fig. 3 shows helium gas permeation reduction at 1 psig of sol gel impregnated samples as a percentage of the as-sprayed values, after 1 and 2 sol layer applications and subsequent firing to 500 °C. Fig. 3 shows the differences in gas permeation for different sol and slurry concentrations, as well as a comparison between PS coatings produced under low and high energy plasma conditions. During this study, as-sprayed substrates were each spin coated with one layer of either the SG or CSG solutions, then dried for two minutes on a hotplate at 300 °C. Gas permeation was measured, a second layer was applied in the same way as the first, and the permeation was measured again. After these two applications, the samples were heated to 500 and

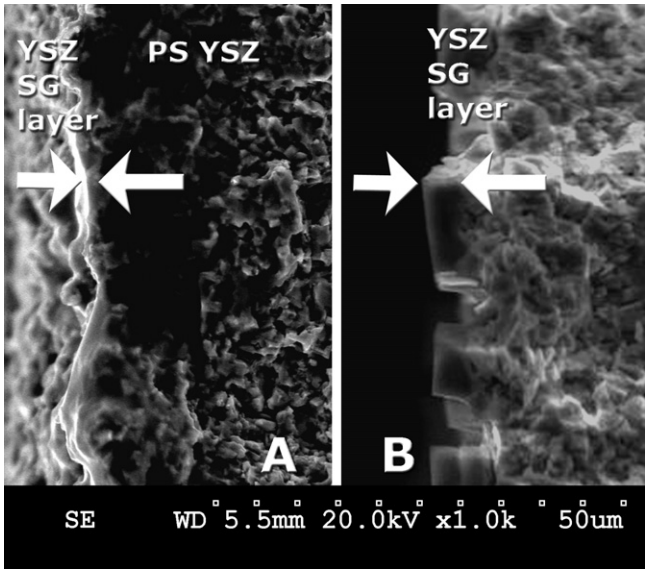

Fig. 2. Cross-section of a fracture surface of high energy PS YSZ electrolytes after 5 (A), and 10 (B) spin coated layers of medium concentration YSZ sol, with each layer dried on a hot plate, followed by a single firing step at 650 °C. The arrows indicate the sol gel surface layer formed.

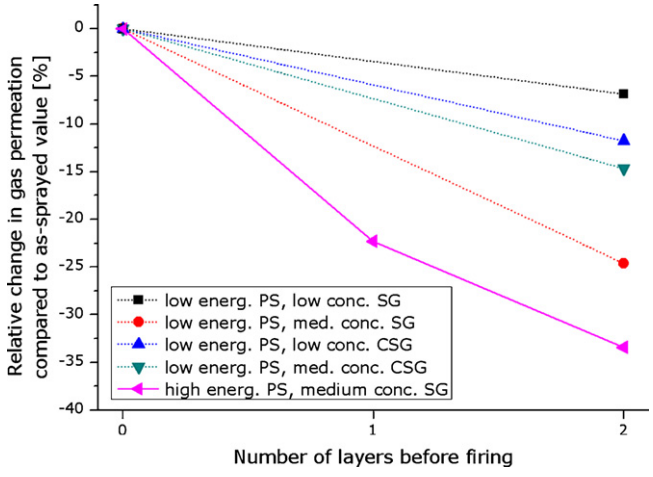

Fig. 3. Relative changes in gas permeation at 1 psig due to sol gel impregnation. Comparison of the effect of the different sol gel solutions and plasma spray coating conditions on gas permeation. Changes are shown as a function of the number of layers coated before firing to 650 °C (low energy plasma samples) and 500 °C (high energy plasma samples).

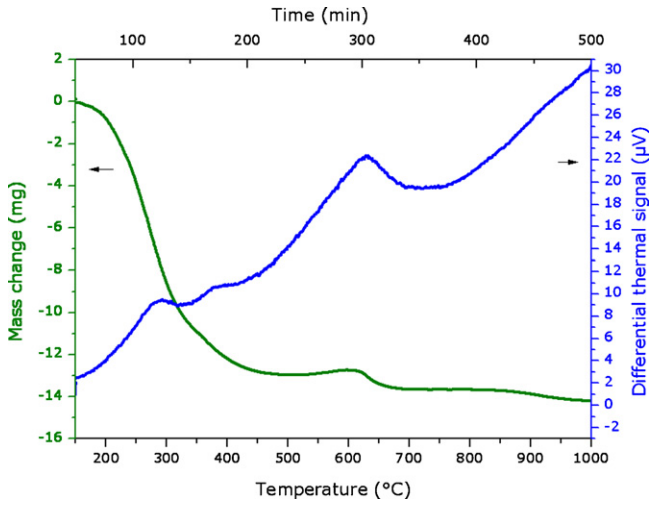

Fig. 4. Thermogravimetric and differential thermal analysis of medium concentration YSZ sol with no powder loading.

650 °C, followed by an additional permeation test after each firing step. While the dried sol gel layers significantly reduced the gas permeation, an effect that increased with the number of layers, the effect became less pronounced after firing to higher temperatures of the sol gel layers. This result may indicate that while initially, the sol derived coatings fill most of the pores present in the PS electrolyte, the sintering shrinkage of the sol after firing at 500 or at 650 °C allows more gas to pass through the electrolyte, albeit less than prior to the sol gel treatment. The permeation reduction achieved after firing ranged from ∼5 to 35% over the range of compositions examined. Higher sol concentrations and composite sol powder loadings did not improve the gas permeation of the PS coatings further compared to the two lower sol concentrations and lowest powder loadings studied.

There was almost no difference visible in permeation between coatings fired to 500 °C and those fired to 650 °C. However, the high sol concentration coatings of both sol gel and composite sol gel layers were visible as a grey layer on top of the sample after firing to 500 °C. This layer appeared white on the surface of the samples after an additional firing step to 650 °C. This behaviour was not observed in any of the other solutions investigated. This observation correlates well with the thermogravimetric results of medium concentration YSZ sol heated to 1000 °C (Fig. 4). A small weight change occurs between 600 and 650 °C, coupled with an exothermic DTA signal. However, the changes that occur between 500 and 650 °C do not affect the gas permeation values significantly.

Fig. 5 shows high-temperature XRD data corresponding to the sol gel reaction that occurs during the low-temperature firing step in processing, as well as during any subsequent further temperature increases at fuel cell operating conditions. The cubic YSZ phase has formed by 650 °C, as seen by the YSZ peaks in the XRD pattern. Further YSZ crystallite growth continues up to 1000 °C. The presence of NiO peaks can be detected at temperatures above 650 °C, resulting from the oxidation of the Ni in the sample holder. These results suggest that a 650 °C firing temperature is sufficient for reacting the sol precursor to form the cubic YSZ phase, with no need for higher temperature sintering steps

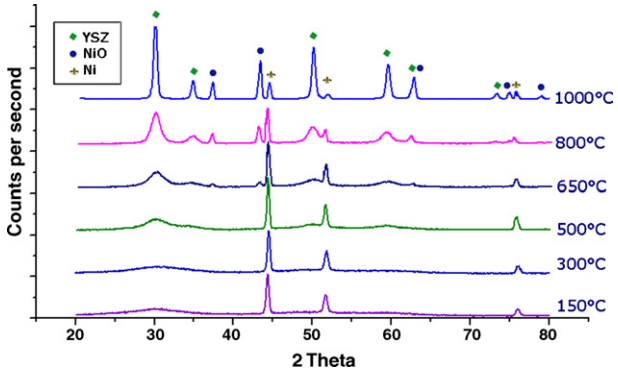

Fig. 5. High-temperature XRD data. NiO peaks appear above 650 °C resulting from oxidation of the Ni sample holder. The YSZ peaks show the progression of crystallization during heating from 150 to 1000 °C.

that would otherwise accelerate oxidation of metallic interconnects or lead to undesired interreactions between the fuel cell layers [30].

Although ex-situ firing of the SG layers was performed in these studies to allow gas permeation testing under different conditions, firing of the sol gel coated layers could potentially be performed in situ prior to fuel cell operation, thus eliminating the need for an additional separate processing step. Since cell operating temperatures with a purely zirconia-based electrolyte are typically above 650 °C, there is the possibility of further sintering of the SG particles in use. However, since no change in gas permeation was observed between firing steps at 500 and 650 °C, after a large change in gas permeation upon firing at 500 °C, it is possible that nano-phase particle sintering within the pores is complete by 500 °C. Studies of in situ sintering of the SG layers at different operating temperatures would provide further insight into the sintering behaviour of the SG layers.

The effects of applying up to five consecutive individually fired SG coatings on the PS electrolytes produced in the hotter plasma conditions are shown in Fig. 6. Up to a total of five coatings continuously decreased the gas permeation, by up to 70%. In this study, each coating of one layer was followed by a

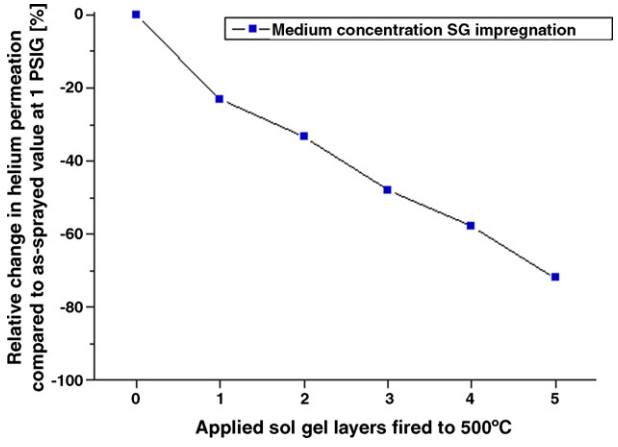

Fig. 6. Normalized gas permeation change through as-sprayed coatings produced in high energy plasma, and after the addition of up to five medium concentration SG coatings, after subsequent firing of each layer individually to 500 °C.

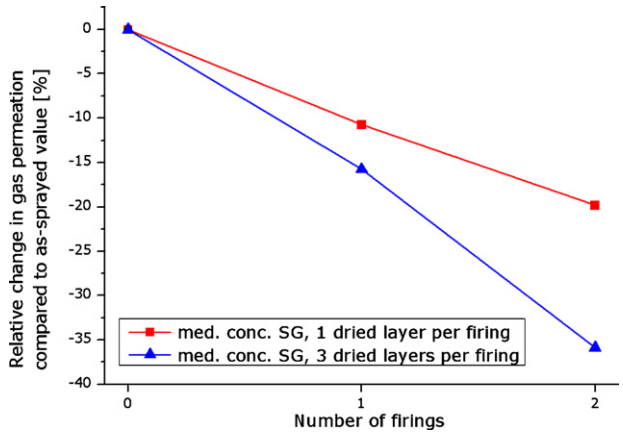

Fig. 7. Normalized gas permeation changes at 1 psig through as-sprayed electrolytes produced in low energy plasma, after two applications of either one or three SG coatings with medium concentration with subsequent firings to 650 °C.

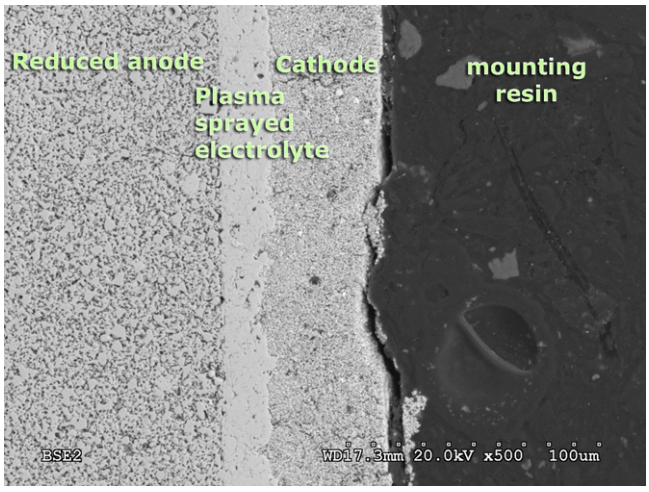

Fig. 8. Backscatter electron image of a full fuel cell after six sol gel impregnation coatings, with a firing step after each third coating, on the electrolyte prior to cathode deposition. The reduced Ni/YSZ anode is shown on the left side, the low energy plasma sprayed YSZ layer is sandwiched in the centre, and the SSC-SDC cathode can be seen to the right of the electrolyte. The dark region on the right of the image is the mounting resin. No separate sol gel film could be discerned in the cross-section.

sintering step to 500 °C. The total reduction of helium permeation was on the order of 16% for one coating and 37% for two coatings after sintering.

An additional variation of the sol gel impregnation method was performed by applying either one, two, or three layers of medium ionic concentration sols by spin coating and hot plate drying on substrates with YSZ coatings produced in a low energy plasma. The samples were then fired to 650 °C. The same number of layers were then coated and heated again to 650 °C. Fig. 7 shows gas permeation results for one or three spin coated films applied and dried on a hot plate prior to a firing step, with and without a repetition of the coating and firing step. The application of two coatings of three layers each with an intermediate firing step results in a 37.5% reduction in gas permeation.

In order to correlate the helium gas leakage through the electrolytes in ex situ tests with the resulting effects on fuel cell performance, electrochemical testing was also performed on the leakage-tested cells. Cathodes were applied to as-sprayed samples with no SG impregnation, and to the samples with 6 dried layers, fired to 650 °C in between two spin coating steps of three dried layers each. The cell setup is shown in Fig. 1, and an SEM micrograph of a fuel cell cross-section is shown in Fig. 8.

The electrochemical impedance spectra of the cells without SG layers and with six medium concentration SG coating layers with two firing steps are shown in Fig. 9. There is a greater than one order of magnitude difference between the polarization resistances (R_P) of the cells, and a smaller difference in series resistances (R_S) of the two cells. The sol-impregnated cell exhibits total cell resistance values ($R_S + R_P$) of 0.56, 1.06, and 2.20 Ωcm^2, while the as-sprayed cell has total cell resistance values of 18.1, 38.7, and 59.8 Ωcm^2 at 800, 750, and 700 °C, respectively.

The OCV of the cells is independent of surface reactions, diffusion, and internal electrical resistance, and thus gives a direct measure of how well the gases are separated from each other. The electrochemically tested cells showed a difference in OCV between the as-sprayed cells and the cells impregnated with six coatings of medium concentration sol and fired after each third coating layer of approximately 0.36 V (Fig. 10). This OCV difference correlates to a difference in gas permeation of 0.279 sccm at 1 psig, a reduction in gas permeation approximately equivalent to 60% of the as-sprayed permeation rate. The impregnated cell remains approximately 0.1 V under the theoretical OCV, while the as-sprayed cells have an OCV of 0.52, 0.46 V below the theoretical OC V at 800 °C.

An as-sprayed cell, with a permeation rate of 0.332 sccm He at 1 psig, exhibited a very poor maximum power density of only 2.2 mW cm^{-2}. Polarization curves at 800, 750, and 700 °C for the cell impregnated with six medium concentration SG coatings fired after every third coating are shown in Fig. 11. The cell produced a maximum power density of 180 mW cm^{-2} at 800 °C, 102 mW cm^{-2} at 750 °C, and 55 mW cm^{-2} at 700 °C. As expected, the OCV increases slightly with lower temperatures, from 0.878 V at 800 °C to 0.894V at 750 °C to 0.914 V

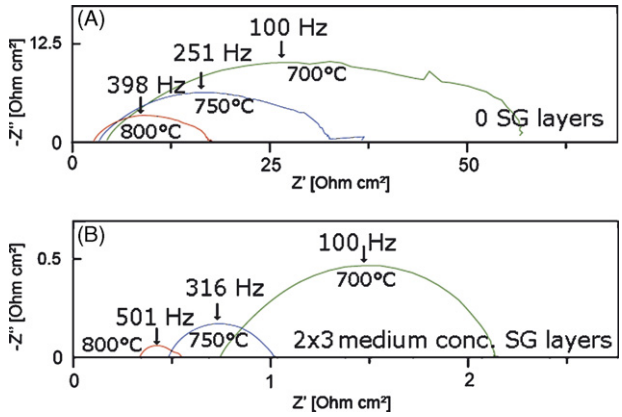

Fig. 9. Impedance spectra of fuel cells with non-impregnated electrolyte layer (top, 1–100 kHz) and with electrolyte layer impregnated with six medium concentration SG layers with two firing steps (bottom, 800 °C: 1–5000 Hz, 750 °C, 1–8500 Hz, 700 °C: 1–10,000 Hz). The fuel cell electrolytes were produced in low energy plasma conditions.

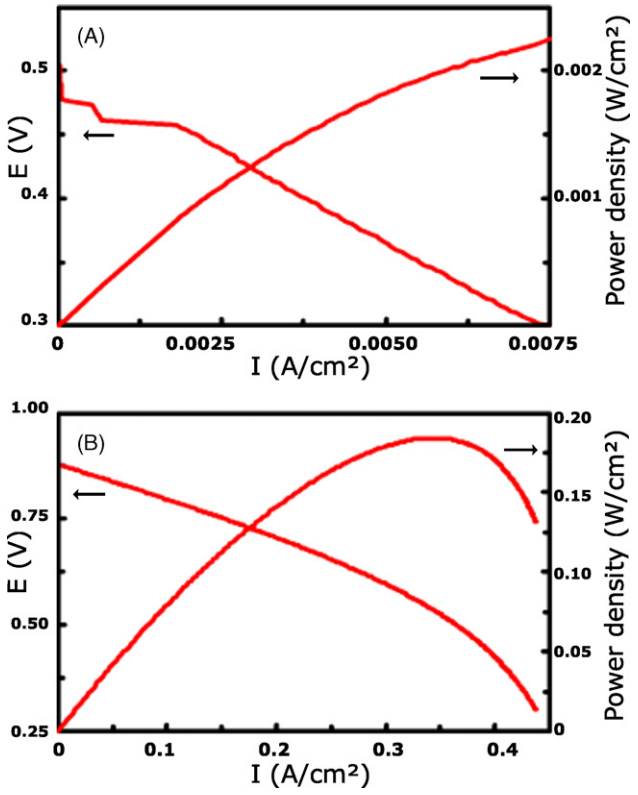

Fig. 10. (A) IV curve at 800 °C of a full fuel cell with an electrolyte layer produced in a low energy plasma without subsequent sol gel impregnation. The performance is compared to that of another cell at 800 °C with six sol gel impregnation steps after PS deposition, fired to 650 °C after every third layer (B).

at 700 °C, at an absolute permeation rate of 0.177 sccm at 1 psig. The absolute values of OCV, however, are approximately 100 mV lower than the theoretical maximum values of 0.980, 0.995, and 1.011 V, at 800, 750, and 700 °C, respectively [31].

Approximately 40 mV of the difference compared to the theoretical values may be attributed to the sealing configuration of the test station used. The remaining 60 mV of OCV loss corresponds to the 0.177 sccm at 1 psig of helium gas leakage through the electrolyte layer in the ex situ gas leakage tests after the application of the SG coatings for sealing. This result suggests that

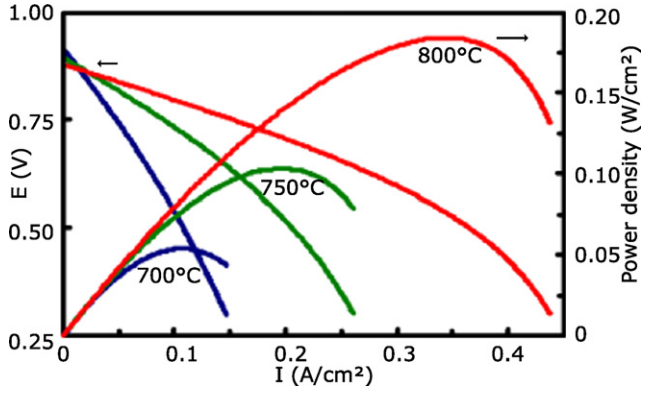

Fig. 11. Full cell performance of a fuel cell with six SG impregnation layers and two firing steps to 650 °C; measured at 800, 750 and 700 °C.

an additional performance increase of approximately 11%, or approximately 20 mW cm^{-2} increase in peak power density at 800 °C, may still be possible through further porosity reduction in either the as-sprayed or SG impregnated coatings.

There are several effects that likely contribute to the electrochemical behaviour shown in Figs. 9–11. Firstly, the SG impregnated cells have a much higher OCV (Fig. 10) and thus a higher voltage at peak power density, resulting in higher performance. Secondly, the electrolyte is denser after impregnation, and thus R_S is slightly lower, as seen in the impedance plots of Fig. 9. Thirdly, the sol gel coatings enhance the sprayed surface by the creation of more numerous and finer cathode reaction sites, thereby resulting in a lower polarization resistance. This effect is quite substantial, as the impedance plots in Fig. 9 indicate a difference in polarization resistance of more than one order of magnitude between the SG-sealed and as-sprayed coatings.

Furthermore, the SG spin coated layers achieved the largest relative reductions in gas permeation rates on the thicker electrolytes produced in the higher energy plasmas. Since electrolytes produced in high energy plasmas have smaller pores, the nanoparticles from the sol are more likely to fill a larger proportion of those pores as compared to larger pores in electrolytes produced in colder plasma conditions. Consequently, in this study, the hotter plasma conditions and thicker electrolytes investigated yielded larger relative improvements in gas permeability by the impregnation process. This result suggests that improvements in the initial porosity of the PS coatings may lead to even larger improvements when combined with the application of SG derived layers.

The SG coatings can lead to significant increases in both gas tightness and interfacial surface area of the electrolytes, without separate high-temperature sintering steps. These improvements result in increases in OCV and peak power density compared to the as-deposited layers, and large reductions in polarization resistance. Although the addition of a spin coated SG layer adds an additional processing step, the potential for improving performance without the need for high-temperature sintering can lead to step changes in cost reduction, for example, by facilitating the use of thinner anode layers while supporting the entire fuel cell on less-expensive metallic interconnects. The present study indicates that with coatings produced in a high energy plasma, the efficiency of the spin coating impregnation is increased, leading to the possibility of using fewer coating steps to improve the density of the plasma sprayed electrolytes.

For cells with thinner electrolytes and thus potentially better electrochemical performance, but higher gas permeation rates, it was shown that the medium concentration sol gel solution was most effective in reducing the gas permeation. It was also shown that three impregnations with intermediate dryings prior to firing could improve the gas tightness more than single applications. The combination of a high energy plasma with a low electrolyte thickness, the application of medium concentration sol without solid loading, and the use of multiple impregnations prior to firing thus would appear likely to yield the best overall result in cell performance for this process.

Further performance improvements could potentially be realized by reducing the porosity of the original PS coatings and

optimizing the SG layers for maximum interfacial reaction surface area. Improvements to process efficiency could potentially be realized by using only in situ firing of the SG layers rather than separate firing steps. Further work is required in these areas to realize the maximum benefits possible from the technique.

4. Conclusions

A method to increase gas tightness in PS YSZ coatings on NiO/YSZ substrates has been presented. Sol gel and composite sol gel spin coating proved to be an easy and fast method to deposit layers on the PS surface. The technique reduced the gas permeation through the electrolyte layers by up to 37% after firing to 500 or 650 °C. High energy plasma conditions provided increased gas tightness of YSZ electrolytes after sol gel impregnation compared to electrolytes produced in low energy plasmas. The SG coatings led to a substantial increase in OCV and a small decrease in series resistance due to the decreased porosity of the electrolytes. The SG coatings also led to increased interfacial surface area, resulting in a large decrease in polarization resistance. These changes resulted in a substantial increase in peak power density. Although the present technique increases the steps necessary to create a fuel cell, the OCV and cell performance are significantly increased, while still avoiding the need for high-temperature sintering. As a result, the primary benefits of the PS process for producing SOFCs are preserved.

Acknowledgements

The authors gratefully acknowledge assistance with electrochemical testing by Cyrille Decès-Petit of NRC-IFCI, with plasma spraying by Zbigniew Celler of Northwest Mettech, Bradley White, David Waldbillig, and Rudy Cardeno, and with powder preparation by Paolo Marcazzan, all of UBC. The precursor work of Mehrdad Keshmiri, UBC, is also gratefully acknowledged. The cathode slurry was graciously supplied by Xinge Zhang of NRC-IFCI. The authors furthermore would like to graciously express their thanks to Brad Thompson, Cancarb Ltd., Medicine Hat, Canada for providing the carbon powders, and for funding by the Canadian Natural Sciences and Engineering Research Council (NSERC).

References

[1] Y. Zhang, X. Huang, Z. Lu, X. Ge, J. Xu, X. Xin, X. Sha, W. Su, Solid State Ionics 177 (3–4) (2006) 281–287.
[2] H.B. Guo, R. Vaßen, D. Stoever, Surf. Coat. Technol. 186 (2004) 353–363.
[3] Y.Y. Chen, W.C.J. Wei, Solid State Ionics 177 (3–4) (2006) 351–357.
[4] O. Kesler, Mater. Sci. Forum 539–543 (2007) 1385–1390.
[5] K.T. Scott, J.L. Woodhead, Proc. Int. Conf. Metallurg. Coat. Proc. Technol., San Diego, CA, USA, April 5–8, 1982, pp. 219–225.
[6] O. Kesler, J. Matejick, S. Sampath, S. Suresh, T.G. Herold, P.C. Brand, H.J. Prask, Mater. Sci. Eng. A 257 (2) (1998) 215–224.
[7] T. Troczynski, S. Cockroft, H. Wong, Key Eng. Mater. 122–124 (1996) 451–462.
[8] E. Fendler, R. Henne, M. Lang, Proc. 8th Nat. Therm. Spray Conf., Houston, Texas, September 11–15, 1995, pp. 533–537.
[9] P. Fauchais, J. Phys. D: Appl. Phys. 37 (2004) R86–R108.
[10] R. Hui, Z. Wang, O. Kesler, L. Rose, J. Jankovic, S. Yick, R. Maric, D. Ghosh, Thermal plasma spray for SOFCs: application, potential advantages and challenges, J. Power Sources (submitted for publication).
[11] S. Jiansirisomboon, K.J.D. MacKenzie, S.G. Roberts, P.S. Grant, J. Eur. Ceram. Soc. 23 (2003) 961–976.
[12] R. Vaßen, N. Czech, W. Malléner, W. Stamm, D. Stöver, Surf. Coat. Technol. 141 (2–3) (2001) 135–140.
[13] T. Goto, Solid State Ionics 172 (1–4) (2004) 225–229.
[14] G. John, T. Troczynski, in: C.C. Berndt (Ed.), Proc. 9th Nat. Thermal Spray Conf., Cincinnati, October 7–11, 1996, ASM International, Ohio, 1996, pp. 483–489.
[15] J. Oberste-Berghaus, S. Bouaricha, J.G. Legoux, C. Moreau, Proc. Int. Therm. Spray Conf., ITSC 2005, Bâle, Switzerland, May 2–4, 2005, CD-Rom, DVS Verlag GmbH, Dusseldorf, Germany, 2005, 6 pages.
[16] P. Bianchi, F. Cernuschi, L. Lorenzoni, S. Ahmaniemi, M. Vippola, P. Vuoristo, T. Mäntylä, in: J. Lecomte-Beckers et al. (Eds.), Proc. 7th Liege Conf. Mater. Adv. Power Eng., Energy Technol. 21 (2002) 449–463.
[17] S. Ahmaniemi, P. Vuoristo, T. Mantyla, Surf. Coat. Technol. 151–152 (2002) 412–417.
[18] S. Ahmaniemi, P. Vuoristo, T. Mäntylä, C. Gualco, A. Bonadei, R. Di Maggio, Surf. Coat. Technol. 190 (2005) 378–387.
[19] B.R. Marple, J. Voyer, P. Bechard, J. Eur. Ceram. Soc. 21 (2001) 861–868.
[20] K.A. Khor, L. Yu, S.H. Chan, X.J. Chen, J. Eur. Ceram. Soc. 23 (2003) 15–18.
[21] X.J. Ning, C.X. Li, C.J. Li, G.J. Yang, Mater. Sci. Eng. A 428 (2006) 98–105.
[22] C.J. Li, X.J. Ning, C.X. Li, Surf. Coat. Technol. 190 (2005) 60–64.
[23] D. Raybould, T.E. Strangman, P. Chipko, US patent 2006/0068189 (2006).
[24] R.L. Jones, D. Mess, Surf. Coat. Technol 86–87 (1996) 94–101.
[25] L. Rose, M. Menon, K. Kammer, O. Kesler, P.H. Larsen, Adv. Mater. Res. 15–17 (2007) 293–299.
[26] S. Komarneni, R. Roy, Mater. Lett. 3 (4) (1985) 165–167.
[27] P.G. Keech, D.E. Trifan, V.I. Birss, J. Electrochem. Soc. 152 (3) (2005) A645–A651.
[28] M. Keshmiri, O. Kesler, Acta Materialia 54 (2006) 4149–4157.
[29] Previously unpublished results.
[30] L. Rose, J. Danish Ceram. Soc. 7 (1) (2005) 16.
[31] J. Larminie, A. Dicks, Fuel Cell Systems Explained, second ed., John Wiley & Sons, 2003.